Thermal Stability of Thin Rectangular Plates with Variable Thickness Made of Functionally Graded Materials

M. Pouladvand[*]

Faculty of Engineering, University of Applied Science and Technology, Borojerd Branch, Iran

ABSTRACT

In this research, thermal buckling of thin rectangular plate made of Functionally Graded Materials (FGMs) with linear varying thickness is considered. Material properties are assumed to be graded in the thickness direction according to a simple power law distribution in terms of the volume fractions of the constituents. The supporting condition of all edges of such a plate is simply supported. The equilibrium and stability equations of a FGM rectangular plate (FGRP) under thermal loads derived based on classical plate theory (CPT) via variational formulation, and are used to determine the pre-buckling forces and the governing differential equation of the plate. The buckling analysis of a functionally graded plate is conducted using; the uniform temperature rise, having temperature gradient through-the-thickness, and linear temperature variation in the thickness and closed-form solutions are obtained. The buckling load is defined in a weighted residual approach. In a special case the obtained results are compared by the results of functionally graded plates with uniform thickness. The influences of the plate thickness variation and the edge ratio on the critical loads are investigated. Finally, different plots indicating the variation of buckling load vs. different gradient exponent k, different geometries and loading conditions were obtained.

© 2009 IAU, Arak Branch. All rights reserved.

Keywords: Thermal buckling; FGM plates; Thin rectangular Plate; Classical plate theory; Variable thickness plate; Galerkin method

1 INTRODUCTION

FUNCTIONALLY graded materials (FGMs) have received considerable attention in many engineering applications since they were first reported in 1984 in Japan [1]. Functionally graded material (FGMs) is a mixture in which material properties vary smoothly or continuously from one surface to the other. This continuous change in composition takes advantage of the attractive features of each of its constituents. Typically, these materials are made from a blend of ceramic and metal, or a combination of different metals. The advantage to use these materials bears on this idea that they are able to withstand high-temperature gradient environments while their structural integrity remains intact. For example, the ceramic constituent of the material provides the high-temperature resistance due to its low thermal conductivity. While the ductile metal component prevents the mixture from fracture due to thermal stresses. Furthermore, a mixture of ceramic and metal with a continuously varying volume fraction can be easily manufactured. Due to these advantages, FGMs have been introduced, applied and used in many engineering parts. The non-uniform matter can help the designer to reduce the weight of the structure. Hence, for cases where reduction of weight is of high importance, such as space structures, plates made of FGM material are the best choice however, the buckling load for these plates is a key factor in the design procedure. Moreover, while the problem of the influence of thickness variation on the buckling load has received sufficient attention, still remains open for further debate. Fuchiyama and Noda [2] developed computer programs that analyzed

_____

[*] *E-mail address*: mpoulad@yahoo.com.

the transient heat transfer and the transient thermal stress of a FGM plate, composed of ZrO_2 and Ti-6AI-4v, by the finite element method. Tanigawa et al. [3] derived a one-dimensional temperature solution for a non-homogeneous plate in transient state and also optimized the material composition by introducing a laminated composite model. Analytical formulation and numerical solution of the thermal stress and deformations for axisymmetrical shells of FGM subjected to thermal loading due to fluid was obtained by Takezono et al. [4]. Aboudi et al. developed a new kind of higher order shear deformation theory for functionally graded materials that explicitly couples the micro-structural and macro-structural effects [5]. Reddy and Chin [6] analyzed the dynamic thermoelastic response of functionally graded cylinders and plates. In this work the thermo-mechanical coupling was included in the formulation and a finite element model was used for the formulation. Reddy and Cheng [7] studied three-dimensional thermo-mechanical deformations of a simply supported Monel-zirconia functionally graded rectangular plate by using an asymptotic method. The local effective material properties were estimated by the Mori-Tanaka scheme. Cheng and Batra [8] obtained a new closed form solution for the thermo-mechanical deformations of an isotropic linear thermo-elastic functionally graded elliptic plate rigidly clamped at the edges. The method of asymptotic expansion was used to study three-dimensional mechanical deformations and the deformations due to thermal loads were found in a straightforward manner. Javaheri and Eslami [9, 10] presented the thermal buckling of uniform thickness rectangular FGM plates based on first and higher order plate theories subjested to four types of thermal loads. Najafizadeh and Eslami [11] discussed the thermal buckling of FGM circular plates. The thermal buckling load of the circular plate under uniform temperature rise, thermal gradient across the thickness, and thermal gradient across the radius are derived. Najafizadeh and Heydari [12] presented the thermal buckling of circular FGM plates based on higher order plate theories subjected to two types of thermal loads.

To date and based on conducted literature searches, it became obvious that no studies have been performed on any types of FGM plates with variable thickness. Therefore, in the present article, a thin rectangular FGM plate with linearly varying thickness under three types of thermal loads is considered. Based on the classical plate theory, equilibrium and stability equations are obtained using energy method. Thermal properties are given by a power law, function of z coordinate. To formulate the thermal buckling load, the Galerkin method has been employed. The analysis is based on the governing differential equation of the thin rectangular plate with linear varying thickness and the critical thermal buckling load is derived by the Galerkin method. Resulting equation are used to obtain the closed-form solution for the critical buckling temperature. The influence of the thickness non-uniformly parameter and the edge ratio to the critical load is investigated.

2   FGM PLATE AND ITS PROPERTIES

Consider a FGM thin rectangular plate made from a mixture of ceramics and metals and subjected to a kind of thermal load. The plate coordinate system (x, y, z) is chosen such that; x and y are in-plane coordinates and z is in the direction of the inward normal to the middle surface, the corresponding displacement designated by u, v and w, respectively. The origin of the coordinate system is located at the corner of the plate on the middle plate. The plate side length in the $x-$ direction is designated as a, and b is the length in the $y-$ direction. The thickness of the plate, h, varies in the x, y directions such that (see Fig. 1)

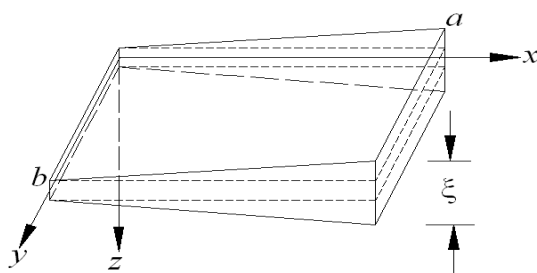$$h = h(x) = \xi = c_1 x + c_2 , \qquad h = h(y) = \xi = c_1 y + c_2 \tag{1}$$

Fig. 1.
Geometry and coordinate system of rectangular plate
$(a \times b)$.

in which ξ is a general parameter indicating the thickness change in either of x or y directions, c_2 is the nominal thickness of the plate at the origin and c_1 is a variable parameter called the non-dimensional parameter. When $c_1 = 0$, that means the plate has a constant thickness. When $x=0$, one has $\xi(0) = c_2 = h$ and for the case of $x=a$, $\xi(a) = c_1 a + c_2$. We assume that the plate composition is varied from the outer to the inner surface, i.e. the outer surface of the plate is ceramic-rich whereas the inner surface is metal-rich. The material properties of the FGM plate, such as coefficient of thermal expansion α, modulus elasticity E, and coefficient of thermal conduction K are assumed to be function of the constituent materials [13]. While the Poisson's ratio ν is assumed to be constant across the plate thickness [14] such that

$$E(z) = E_c V_c + E_m (1 - V_c) \tag{2a}$$

$$\alpha(z) = \alpha_c V_c + \alpha_m (1 - V_c) \tag{2b}$$

$$K(z) = K_c V_c + K_m (1 - V_c) \tag{2c}$$

$$\nu(z) = \nu \tag{2d}$$

where subscripts m and c refer to the metal and ceramic constituents, respectively; the volume fractions of ceramic V_c and metal V_m are related by [15]

$$V_c = (z/h + 1/2)^k, \quad k \geq 0, \tag{3a}$$

$$V_m(z) + V_c(z) = 1 \tag{3b}$$

where volume fraction exponent k dictates the material variation profile through the plate thickness which takes values greater than or equal to zero. The value of zero for the k represents a fully ceramic plate. From Eqs. (2) and (3) material properties of the FGM plate are determined, which are the same as the equations proposed by reference [15]

$$E(z) = E_m + E_{cm}(z/h + 1/2)^k \tag{4a}$$

$$\alpha(z) = \alpha_m + \alpha_{cm}(z/h + 1/2)^k \tag{4b}$$

$$K(z) = K_m + K_{cm}(z/h + 1/2)^k \tag{4c}$$

$$\nu(z) = \nu \tag{4d}$$

in which

$$E_{cm} = E_c - E_m, \quad \alpha_{cm} = \alpha_c - \alpha_m, \quad K_{cm} = K_c - K_m, \tag{5}$$

3   BASIC AND EQUILIBRIUM EQUATIONS

The classical plate theory (CPT) which is considered for further study in the present work is based on the assumption of the displacement field in the following form

$$\begin{aligned} u(x,y,z) &= u_0(x,y) - z w_{0,x} \\ v(x,y,z) &= v_0(x,y) - z w_{0,y} \\ w(x,y,z) &= w_0(x,y) \end{aligned} \tag{6}$$

in which u, v, w are the total displacement and (u_0, v_0, w_0) are the mid-plane displacements in the x, y and z directions, respectively. For the thin plate i.e. $(h/b) \leq (1/20)$, where h and b are the thickness and smaller edge side of the rectangular plate, respectively. Hook's law for a plate with thermal effects is defined as

$$\overline{\sigma}_{xx} = \frac{E(z)}{1-v^2}\left[\overline{\varepsilon}_{xx} + v\overline{\varepsilon}_{yy} - (1+v)\alpha\mathrm{T}\right]$$

$$\overline{\sigma}_{yy} = \frac{E(z)}{1-v^2}\left[\overline{\varepsilon}_{yy} + v\overline{\varepsilon}_{xx} - (1+v)\alpha\mathrm{T}\right]$$

$$\overline{\tau}_{xy} = \frac{E(z)}{2(1+v)}\overline{\gamma}_{xy} \tag{7}$$

The plate is assumed to be comparatively thin and according to the Love-Kirchhoff assumption, normal to the median surface are assumed to remain straight and normal during deformation, thus out-of-plane shear deformations $(\gamma_{xz}, \gamma_{yz})$ are disregarded. Strain components at distance z from the middle plane are then given by

$$\overline{\varepsilon}_{xx} = \varepsilon_{xx} + z\kappa_{xx}$$

$$\overline{\varepsilon}_{yy} = \varepsilon_{yy} + z\kappa_{yy}$$

$$\overline{\gamma}_{xy} = \gamma_{xy} + 2z\kappa_{xy} \tag{8}$$

Here $\varepsilon_{xx}, \varepsilon_{yy}, \gamma_{xy}$ denote the corresponding quantities at points on the mid-plane surface only, and $\kappa_{xx}, \kappa_{yy}, \kappa_{xy}$ are the curvatures which can be expressed in term of the displacement components. The relations between the mid-plane strains and the displacement components according to the Sander's assumption are [16]

$$\varepsilon_{xx} = u_{,x} + \frac{1}{2}w_{,x}^2$$

$$\varepsilon_{yy} = v_{,y} + \frac{1}{2}w_{,y}^2$$

$$\gamma_{xy} = u_{,y} + v_{,x} + w_{,x}w_{,y} \tag{9}$$

and

$$\kappa_{xx} = -w_{,xx}, \qquad \kappa_{yy} = -w_{,yy}, \qquad \kappa_{xy} = -w_{,xy} \tag{10}$$

Substituting Eqs. (9) and (10) into Eqs. (8), the following expression for the strain components are obtained

$$\overline{\varepsilon}_{xx} = u_{,x} + \frac{1}{2}w_{,x}^2 - zw_{,xx}$$

$$\overline{\varepsilon}_{yy} = v_{,y} + \frac{1}{2}w_{,y}^2 - zw_{,yy}$$

$$\overline{\gamma}_{xy} = u_{,y} + v_{,x} + w_{,x}w_{,y} - 2zw_{,xy} \tag{11}$$

A loaded plate is in equilibrium if its total potential energy V remains stationary $(\delta V = 0)$, and V is stationary if the integrand in expression for V satisfies the Euler equations. The total potential energy V of a plate subjected to thermal loads is defined as

$$V = U_m + U_b + U_c + U_T \tag{12}$$

where U_m is the membrane strain energy, U_b is the bending strain energy, U_c is the coupled strain energy, and U_T is the thermal strain energy. The strain energy for thin rectangular plate based on classical plate theory is defined as

$$U = \frac{1}{2} \iiint [\bar{\sigma}_{xx}(\bar{\varepsilon}_{xx} - \alpha T) + \bar{\sigma}_{yy}(\bar{\varepsilon}_{yy} - \alpha T) + \bar{\tau}_{xy}\bar{\gamma}_{xy}]\, dx\, dy\, dz \tag{13}$$

Substituting of Eqs. (7) and (8) into Eq. (13), integration with represent to z from $-\xi/2$ to $\xi/2$, the total potential energy results in

$$V = \iint F\, dx\, dy \tag{14}$$

where functional F is

$$F = \frac{A}{2(1-\nu^2)}\left[\varepsilon_{xx}^2 + \varepsilon_{yy}^2 + 2\nu\varepsilon_{xx}\varepsilon_{yy} + \frac{1-\nu}{2}\gamma_{xy}^2\right] + \frac{C}{2(1-\nu^2)}\left[\kappa_{xx}^2 + \kappa_{yy}^2 + 2\nu\kappa_{xx}\kappa_{yy} + 2(1-\nu)\kappa_{xy}^2\right] +$$

$$\frac{B}{1-\nu^2}\left[\varepsilon_{xx}\kappa_{xx} + \varepsilon_{yy}\kappa_{yy} + \nu(\varepsilon_{xx}\kappa_{yy} + \varepsilon_{yy}\kappa_{xx}) + (1-\nu)\gamma_{xy}\kappa_{xy}\right] - \frac{1}{1-\nu}[\Theta(\varepsilon_{xx} + \varepsilon_{yy}) + \Phi(\kappa_{xx} + \kappa_{yy}) - \psi] \tag{15}$$

where

$$A = \int_{-\xi/2}^{\xi/2} E(z)\, dz = E_m\xi + E_{cm}\frac{\xi}{k+1}$$

$$B = \int_{-\xi/2}^{\xi/2} E(z)z\, dz = E_{cm}\frac{k\xi^2}{(2k+2)(k+2)}$$

$$C = \int_{-\xi/2}^{\xi/2} E(z)z^2\, dz = E_m\frac{\xi^3}{12} + E_{cm}\xi^3\left[\frac{1}{k+3} - \frac{1}{k+2} + \frac{1}{4k+4}\right] \tag{16}$$

$$(\Theta, \Phi) = \int_{-\xi/2}^{\xi/2} (1,z)E(z)\alpha(z)T(x,y,z)\, dz$$

$$\psi = \int_{-\xi/2}^{\xi/2} E(z)\alpha^2(z)T^2(x,y,z)\, dz$$

The total potential energy is a function of the displacement components and their derivatives. Hence, minimization of total potential energy in terms of the functional F yields the following Euler equations [16]

$$\frac{\partial F}{\partial u} - \frac{\partial}{\partial x} \cdot \frac{\partial F}{\partial u_{,x}} - \frac{\partial}{\partial y} \cdot \frac{\partial F}{\partial u_{,y}} = 0 \tag{17a}$$

$$\frac{\partial F}{\partial v} - \frac{\partial}{\partial x} \cdot \frac{\partial F}{\partial v_{,x}} - \frac{\partial}{\partial y} \cdot \frac{\partial F}{\partial v_{,y}} = 0 \tag{17b}$$

$$\frac{\partial F}{\partial w} - \frac{\partial}{\partial x} \cdot \frac{\partial F}{\partial w_{,x}} - \frac{\partial}{\partial y} \cdot \frac{\partial F}{\partial w_{,y}} + \frac{\partial^2}{\partial x^2} \cdot \frac{\partial F}{\partial w_{,xx}} + \frac{\partial^2}{\partial x \partial y} \cdot \frac{\partial F}{\partial w_{,xy}} + \frac{\partial^2}{\partial y^2} \cdot \frac{\partial F}{\partial w_{,yy}} = 0 \tag{17c}$$

Substituting of Eqs. (9) and (10) into Eqs. (15) and using Eqs. (17) the equilibrium equations for general rectangular plate made of functionally graded material are given by

$$N_{x,x} + N_{xy,y} = 0$$
$$N_{xy,x} + N_{y,y} = 0$$
$$M_{x,xx} + 2M_{xy,xy} + M_{y,yy} + N_x w_{,xx} + 2N_{xy}w_{,xy} + N_y w_{,yy} + P_n = 0 \tag{18}$$

where stress resultant N_i, M_i are given by

$$(N_i, M_i) = \int_{-\xi/2}^{\xi/2} (1, z) \cdot \overline{\sigma}_i \cdot dz, \quad i = x, y, xy.$$ (19)

By substitution Eq. (7) into Eq. (19), one can arrive to the following constitutive relation as

$$(N_x, M_x) = \frac{1}{1-\nu^2} \big[(A, B)(\varepsilon_{xx} + \nu\varepsilon_{yy}) + (B, C)(\kappa_{xx} + \nu\kappa_{yy}) - (1+\nu)(\Theta, \Phi) \big]$$

$$(N_y, M_y) = \frac{1}{1-\nu^2} \big[(A, B)(\varepsilon_{yy} + \nu\varepsilon_{xx}) + (B, C)(\kappa_{yy} + \nu\kappa_{xx}) - (1+\nu)(\Theta, \Phi) \big]$$ (20)

$$(N_{xy}, M_{xy}) = \frac{1}{2(1+\nu)} \big[(A, B)\gamma_{xy} + 2(B, C)\kappa_{xy} \big]$$

4 PLATE STABILITY EQUATIONS

Stability equations of thin rectangular plates are derived using the energy method. If V is the total potential energy of the plate, the expanding V about the equilibrium state using Taylor series yields;

$$\Delta V = \delta V + \frac{1}{2!} \delta^2 V + \frac{1}{3!} \delta^3 V + \cdots$$ (21)

The first variation δV is associated with the state of equilibrium. The stability of the plate in the neighborhood of equilibrium condition may be determined by the sign of second variation. The condition $\delta^2 V = 0$ is used to derive the stability equations for buckling problems [16]. Let us assume that $\hat{u}_i$ denotes the displacement component of the equilibrium state and $\delta \hat{u}_i$ the virtual displacement corresponding to a neighboring state. Denoting $\overline{\delta}$ the variation with respect to $\hat{u}_i$, the following rule, known as the Trefftz rule, is stated for the determination of the critical load. The external load acting on the plate is considered to be the critical buckling load if the following variational equation is satisfied $\overline{\delta}(\delta^2 V) = 0$. Consider the state of primary equilibrium of a rectangular plate under general loading to be designated by u_o, v_o, w_o. For derived stability equations, virtual displacements are defined as

$$u \rightarrow u_0 + u_1$$
$$v \rightarrow v_0 + v_1$$ (22)
$$w \rightarrow w_0 + w_1$$

where u_1, v_1, w_1 are the virtual displacement increments. Substituting Eqs. (22) into Eq. (15) and collecting the second-order terms, we obtain the second variation of the potential energy as

$$\begin{aligned}
\frac{1}{2}\delta^2 V = \iint \Bigg\{ &\frac{A}{2(1-\nu^2)}\bigg[u_{1,x}^2 + v_{1,y}^2 + 2\nu u_{1,x}v_{1,y} + \frac{1-\nu}{2}\big(u_{1,y} + v_{1,x} \big)^2 \bigg] - \\
&\frac{B}{1-\nu^2}\Big[u_{1,x}w_{1,xx} + v_{1,y}w_{1,yy} + \nu\big(u_{1,x}w_{1,yy} + v_{1,y}w_{1,xx} \big) + (1-\nu)\big(u_{1,y} + v_{1,x} \big)w_{1,xy} \Big] + \\
&\frac{C}{2(1-\nu^2)}\Big[w_{1,xx}^2 + w_{1,yy}^2 + 2\nu w_{1,xx}w_{1,yy} + 2(1-\nu)w_{1,xy}^2 \Big] + \\
&\frac{1}{2}\Big[N_x^0 w_{1,x}^2 + 2N_{xy}^0 w_{1,x}w_{1,y} + N_y^0 w_{1,y}^2 \Big] \Bigg\} \, dx \, dy
\end{aligned}$$ (23)

Applying the Euler equations (17) to the functional of Eq. (23), we find the stability equations as

$$
N_{x1,x} + N_{xy1,y} = 0
$$
$$
N_{xy1,x} + N_{y1,y} = 0
$$
$$
M_{x1,xx} + 2M_{xy1,xy} + M_{y1,yy} + (N_x^o w_{1,xx} + 2N_{xy}^o w_{1,xy} + N_y^o w_{1,yy}) = 0
$$
(24)

where

$$
(N_{x1}, M_{x1}) = \frac{1}{1-v^2}\Big[(A,B)(u_{1,x} + vv_{1,y}) - (B,C)(w_{1,xx} + vw_{1,yy})\Big]
$$

$$
(N_{y1}, M_{y1}) = \frac{1}{1-v^2}\Big[(A,B)(v_{1,y} + vu_{1,x}) - (B,C)(w_{1,yy} + vw_{1,xx})\Big]
$$

$$
(N_{xy1}, M_{xy1}) = \frac{1}{2(1+v)}\Big[(A,B)(u_{1,y} + v_{1,x}) - 2(B,C)w_{1,xy}\Big]
$$

$$
N_x^0 = \frac{1}{1-v^2}\Big[A(u_{0,x} + vv_{0,y}) - B(w_{0,xx} + vw_{0,yy})\Big] - \frac{\Theta}{1-v}
$$

$$
N_y^0 = \frac{1}{1-v^2}\Big[A(v_{0,y} + vu_{0,x}) - B(w_{0,yy} + vw_{0,xx})\Big] - \frac{\Theta}{1-v}
$$

$$
N_{xy}^0 = \frac{A}{2(1+v)}(u_{0,y} + v_{0,x}) - \frac{B}{1+v}w_{0,xy}
$$
(25)

4.1 Governing differential equation for functionally graded rectangular plate (FGRP)

By substituting Eq. (25) into Eq. (24), the stability equations in terms of displacement components become

$$
A_{,x}(u_{1,x} + vv_{1,y}) + A(u_{1,xx} + vv_{1,xy}) - B_{,x}(w_{1,xx} + vw_{1,yy}) - B(w_{1,xxx} + vw_{1,xyy})
$$
$$
+ \frac{A(1-v)}{2}(u_{1,yy} + v_{1,xy}) - B(1-v)w_{1,xy} = 0
$$
(26a)

$$
\frac{1-v}{2}A_{,x}(u_{1,y} + v_{1,x}) + A\frac{1-v}{2}(u_{1,xy} + v_{1,xx}) - (1-v)B_{,x}w_{1,xy} - (1-v)Bw_{1,xxy}
$$
(26b)
$$
+ A(v_{1,yy} + vu_{1,xy}) - B(w_{1,yyy} + vw_{1,xxy}) = 0
$$

$$
B_{,xx}(u_{1,x} + vv_{1,y}) + 2B_{,x}(u_{1,xx} + vv_{1,xy}) + B(u_{1,xxx} + vv_{1,xxy}) + B(v_{1,yyy} + vu_{1,xyy})
$$
$$
+ (1-v)B_{,x}(u_{1,yy} + v_{1,xy}) + (1-v)B(u_{1,xyy} + v_{1,xxy}) - C_{,xx}(w_{1,xx} + vw_{1,yy})
$$
$$
- 2C_{,x}(w_{1,xxx} + vw_{1,xyy}) - 2C_{,x}(1-v)w_{1,xy} - 2(1-v)Cw_{1,xxyy} - C(w_{1,xxxx} + vw_{1,xxyy})
$$
(26c)
$$
- C(w_{1,yyyy} + vw_{1,xxyy}) + (1-v^2)[N_x^0 w_{1,xx} + N_y^0 w_{1,yy} + 2N_{xy}^0 w_{1,xy}] = 0
$$

In the next step we eliminate variables u, v in above relations; then the equations of stability (26) can be merged into one equation in terms of deflection component w and pre-buckling forces only for linear thickness variation as

$$
\left(\frac{B^2}{A} - C\right)\Delta\Delta w_1 + \left(3\frac{B}{A}B_{,x} - 2C_{,x}\right)\frac{\partial}{\partial x}\Delta w_1 + \left(\frac{B}{A}B_{,xx} + \frac{B_{,x}^2}{A} - C_{,xx}\right)(w_{1,xx} + vw_{1,yy})
$$
(27)
$$
+ (1-v^2)\left(N_x^0 w_{1,xx} + N_y^0 w_{1,yy} + 2N_{xy}^0 w_{1,xy}\right) = 0
$$

where

$$\Delta = \frac{\partial^2}{\partial x^2} + \frac{\partial^2}{\partial y^2} \tag{28}$$

4.2 Solution method

The method of solving Eq. (27) is based on the series expansion developed by Galerkin [16]. It was originally proposed by Bubnov and sometimes is referred to as the Bubnov-Galerkin method. A brief description of the method is coming in the following. If the FGM rectangular plate is simply supported in all four edges, then the boundary condition is

$$w_1 = 0, \qquad w_{1,xx} = 0 \qquad \text{at} \quad x = 0, a \,,$$
$$w_1 = 0, \qquad w_{1,yy} = 0 \qquad \text{at} \quad y = 0, b \,, \tag{29}$$

The proposed deflection function w_1 for this case is assumed to be in the following series form

$$w_1 = B_{mn} \ \sin(m\pi x / a) \ \sin(n\pi y / b), \ (m,n) = 1,\ 2,\ 3,\dots . \tag{30}$$

where B_{mn} are constant coefficients, and m, n are the half wave numbers in the x, y directions, respectively. In this article, in order to determine the critical load, the Galerkin method is used. According to this method

$$\iint_\Omega \phi(w) R(x,y) \, \mathrm{d}x \, \mathrm{d}y = 0 \,, \tag{31}$$

in which $R(x,y)$ is the residue function and $\phi(w)$ is the weight function.

5   THERMAL BUCKLING ANALYSIS

In this section, the closed form solutions of Eq. (27) for three types of thermal loading conditions are presented. The plate is assumed to be simply supported in all edges and rigidity fixed against any extension.

Case A. *Uniform temperature rises*

The initial uniform temperature of the plate is assumed to be T_i, the temperature can be uniformly raised to final value T_f, such that the plate buckles. To find the critical buckling temperature difference i.e., $\Delta T_A = T_f - T_i$, the pre-buckling thermal forces, should be found. Solving the membrane form of equilibrium equations i.e., Eq (18), gives the pre-buckling force resultants as

$$N_x^0 = -\frac{\Delta T_A G_1}{2(1-\nu)}(c_1 a + 2c_2) \,, \quad N_y^0 = -\frac{\Delta T_A G_1}{2(1-\nu)}(c_1 a + 2c_2) - \Delta T_A G_1 c_1 x \,, \quad N_{xy}^0 = 0 \tag{32}$$

where

$$G_1 = [E_m \alpha_m + (E_m \alpha_{cm} + E_{cm} \alpha_m)/(k+1) + E_{cm} \alpha_{cm} /(2k+1)] \tag{33}$$

By substituting this type of loading in Eqs. (16), one can get

$$\Theta = \Delta T_A \cdot \xi \cdot G_1 \tag{34}$$

Substituting Eq. (32) into Eq. (27), the buckling equation for this type of loading is obtained as

$$\left(\frac{B^2}{A}-C\right)\Delta\Delta w_1+\left(3\frac{B}{A}B_{,x}-2C_{,x}\right)\frac{\partial}{\partial x}\Delta w_1+\left(\frac{B}{A}B_{,xx}+\frac{B_{,x}^2}{A}-C_{,xx}\right)(w_{1,xx}+\nu w_{1,yy})$$
$$-(1-\nu^2)\Delta T_A G_1\left[\left(\frac{c_1a}{2(1-\nu)}+\frac{c_2}{1-\nu}\right)w_{1,xx}+\left(c_1x+\frac{\nu c_1a}{2(1-\nu)}+\frac{c_2}{1-\nu}\right)w_{1,yy}\right]=0$$

(35)

For the assumed displacement field given by Eq. (30) the result of Eqs. (31) and (35) becomes

$$\frac{\pi^2 B_{mn}}{a^4 b^4}\int_0^b\int_0^a\Big\{\pi^2(m^2b^2+n^2a^2)^2(\tilde{B}^2/\tilde{A}-\tilde{C})(c_1x+c_2)^3\sin(m\pi x/a)\sin(n\pi y/b)$$
$$+(6\tilde{B}^2/\tilde{A}-9\tilde{C})mab^2(m^2b^2+n^2a^2)c_1(c_1x+c_2)^2\cos(m\pi x/a)\sin(n\pi y/b)+$$
$$6(\tilde{B}^2/\tilde{A}-\tilde{C})(m^2b^2+\nu n^2a^2)a^2b^2(c_1^3x+c_1^2c_2)\sin(m\pi/a)\sin(n\pi/b)+$$
$$(1-\nu^2)\Delta T_A G_1[(c_1a/2(1-\nu^2)+c_2/(1-\nu))(m\pi/a)^2+(c_1x+\nu c_1a/2(1-\nu)+c_2/(1-\nu))$$
$$(n/b)^2]a^4b^4\sin(m\pi x/a)\sin(n\pi y/b)\Big\}\sin(m\pi x/a)\sin(n\pi y/b)\,dx\,dy=0$$

(36)

After carrying out the integration, one would get

$$\Delta T_A=H.\left[(mb/a)^2+n^2\right]$$

(37)

in which

$$H=\frac{\pi^2}{b^2(1+\nu)(c_1a/2+c_2)G_1}\Big\{(\tilde{C}-\tilde{B}^2/\tilde{A})(c_1^3a^3/4+c_1^2c_2a^2+3c_1c_2^2a/2+c_2^3)$$
$$+6\big(\tilde{C}-\tilde{B}^2/\tilde{A}\big)\frac{a^2b^2(m^2b^2+\nu n^2a^2)}{\pi^2(m^2b^2+n^2a^2)^2}(c_1^3a/2+c_1^2c_2)\Big\}$$

(38)

where

$$\tilde{A}=E_m+E_{cm}/(k+1),\quad \tilde{B}=E_{cm}k/(2k+2)(k+2),$$
$$\tilde{C}=E_m/12+E_{cm}[1/(k+3)-1/(k+2)+1/(4k+4)]$$

(39)

The critical buckling load ΔT_A^{cr} can be obtained for different values of m,n such that it minimizes Eq. (37). Apparently, when minimization methods are used, the critical buckling load, ΔT_A^{cr}, is obtained for $m=n=1$, thus

$$\Delta T_A^{cr}=\frac{\pi^2[(b/a)^2+1]}{b^2(1+\nu)(c_1a/2+c_2)G_1}\Big\{(\tilde{C}-\tilde{B}^2/\tilde{A})(c_1^3a^3/4+c_1^2c_2a^2+3c_1c_2^2a/2+c_2^3)$$
$$+6\big(\tilde{C}-\tilde{B}^2/\tilde{A}\big)\frac{a^2b^2(b^2+\nu a^2)}{\pi^2(b^2+a^2)^2}(c_1^3a/2+c_1^2c_2)\Big\}$$

(40)

when $c_1=0$, Eq. (40) represents the critical thermal buckling load, $\Delta T_{A_i}^{cr}$ of a FGM rectangular plate with constant thickness $c_2=h$, i.e.

$$\Delta T_{A_i}^{cr.} = \frac{\pi^2 \left(\left(\frac{b}{a} \right)^2 + 1 \right)}{b^2(1+\nu)hG_1} \left(\frac{A \cdot C - B^2}{A} \right) \tag{41}$$

The result given in Eq. (41) is exactly the same as the one obtained by Ref. [9].

Case B. *Linear temperature change across the thickness*

For a functionally graded plate, the temperature change is not uniform. Usually, the temperature level is much higher at the ceramic side than that in the metal side of the plate. In this case, the temperature variation through the thickness is given by

$$T(z) = \frac{\Delta T_B}{\xi} (z + \frac{\xi}{2}) + T_m \tag{42}$$

in which

$$\begin{aligned} T \big|_{z=\frac{\xi}{2}} &= T_c \\ T \big|_{z=-\frac{\xi}{2}} &= T_m \\ \Delta T_B &= T_c - T_m \end{aligned} \tag{43}$$

where T_c and T_m denote the temperature level at the top (ceramic side) and the bottom (metal side) surfaces, respectively. The pre-buckling forces now can be obtained by solving the membrane form of equilibrium equations, i.e. Eq. (18) this gives

$$\begin{aligned} N_x^0 &= -\frac{c_1 a/2 + c_2}{1-\nu} (\Delta T_B G_2 + T_m G_1) \\ N_y^0 &= -\left(c_1 x + \frac{\nu c_1 a}{2(1-\nu)} + \frac{c_2}{1-\nu} \right)(\Delta T_B G_2 + T_m G_1), \qquad N_{xy}^0 = 0 \end{aligned} \tag{44}$$

in which

$$G_2 = [E_m \alpha_m / 2 + (E_m \alpha_{cm} + E_{cm} \alpha_m)/(k+2) + E_{cm}\alpha_{cm}/(2k+2)] \tag{45}$$

Substituting Eq. (44) into Eq. (27), buckling equation for this case of loading is obtained

$$\begin{aligned} &\left(\frac{B^2}{A} - C \right) \Delta\Delta w_1 + \left(3\frac{B}{A}B_{,x} - 2C_{,x} \right) \frac{\partial}{\partial x} \Delta w_1 + \left(\frac{B}{A}B_{,xx} + \frac{B_{,x}^2}{A} - C_{,xx} \right)(w_{1,xx} + \nu w_{1,yy}) \\ &- (1-\nu^2) \left[\left(\frac{c_1 a}{2(1-\nu)} + \frac{c_2}{1-\nu} \right) w_{1,xx} + \left(c_1 x + \frac{\nu c_1 a}{2(1-\nu)} + \frac{c_2}{1-\nu} \right) w_{1,yy} \right](\Delta T_B G_2 + T_m G_1) = 0 \end{aligned} \tag{46}$$

By following similar steps to that given in case A, the buckling load for case B is

$$\Delta T_B^{cr} = \frac{\pi^2[(b/a)^2+1]}{b^2(1+v)(c_1a/2+c_2)G_2}\left\{(\widetilde{C}-\widetilde{B}^2/\widetilde{A})(c_1^3a^3/4+c_1^2c_2a^2+3c_1c_2^2a/2+c_2^3)\right.$$

$$\left.+6\left(\widetilde{C}-\widetilde{B}^2/\widetilde{A}\right)\frac{a^2b^2(b^2+va^2)}{\pi^2(b^2+a^2)^2}(c_1^3a/2+c_1^2c_2)\right\}-\frac{T_mG_1}{G_2}$$

(47)

when $c_1=0$, Eq. (47) is reduced to the critical buckling load $\Delta T_{B_i}^{cr}$ of a FGM rectangular plate with constant thickness $c_2=h$, which is

$$\Delta T_{B_i}^{cr.} = \frac{\pi^2[(b/a)^2+1]}{b^2(1+v)hG_2}\left(\frac{A\cdot C-B^2}{A}\right)-\frac{T_mG_1}{G_2}$$

(48)

The result given in Eq. (48) is exactly the same as the one obtained by Ref. [9].

Case C. *Buckling of FGRP under non-linear temperature change across the thickness*

In this section, the governing differential equation for the temperature distribute through the thickness is given by one-dimensional Fourier equation under steady state heat condition as

$$\frac{d}{dz}\left[K(z)\frac{dT}{dz}\right]=0$$

(49)

where $K(z)$ is the coefficient of thermal conduction. Similar to what was considered for the variation of the elastic modulus and coefficient of thermal expansion, here the coefficient of the heat conduction is also assumed to change according to a power law in terms of z as represented by Eq. (4c). By inserting Eq. (4c) into Eq. (49) one would get

$$\frac{d^2T}{dm^2}+\frac{kK_{cm}m^{k-1}}{K_m+K_{cm}m^k}\frac{dT}{dm}=0$$

(50)

in which

$$m=\frac{2z+\xi}{2\xi}$$

(51)

and boundary conditions across the plate thickness are

$$
\begin{aligned}
T&=T_c, & m&=1\\
T&=T_m, & m&=0
\end{aligned}
$$

(52)

The solution of Eq. (50) can be obtained by means of polynomial series. Taking the first seven terms of the series, we have

$$T=\hat{C}_0+\hat{C}_1m+\hat{C}_2m^2+\hat{C}_3m^3+\hat{C}_4m^4+\hat{C}_5m^5+\hat{C}_6m^6$$

(53)

in which $\hat{C}_i$ are constant coefficients to be evaluated. After substituting Eq. (53) into Eq. (50) imposing the boundary conditions and doing some mathematical manipulations, one can get

$$T(z) = T_m + \frac{\Delta T_c}{\hat{C}_0} L(z) \tag{54}$$

in which

$$\hat{C}_0 = 1 - \frac{K_{cm}}{(k+1)K_m} + \frac{K_{cm}^2}{(2k+1)K_m^2} - \frac{K_{cm}^3}{(3k+1)K_m^3} + \frac{K_{cm}^4}{(4k+1)K_m^4} - \frac{K_{cm}^5}{(5k+1)K_m^5} \tag{55a}$$

$$L(z) = \left(\frac{2z+\xi}{2\xi}\right) - \frac{K_{cm}}{(k+1)K_m}\left(\frac{2z+\xi}{2\xi}\right)^{k+1} + \frac{K_{cm}^2}{(2k+1)K_m^2}\left(\frac{2z+\xi}{2\xi}\right)^{2k+1}$$

$$- \frac{K_{cm}^3}{(3k+1)K_m^3}\left(\frac{2z+\xi}{2\xi}\right)^{3k+1} + \frac{K_{cm}^4}{(4k+1)K_m^4}\left(\frac{2z+\xi}{2\xi}\right)^{4k+1} - \frac{K_{cm}^5}{(5k+1)K_m^5}\left(\frac{2z+\xi}{2\xi}\right)^{5k+1} \tag{55b}$$

$$\Delta T_c = T_c - T_m \tag{55c}$$

The pre-buckling resultants loads for this case can be obtained by solving the membrane form of equilibrium equations i.e., (Eq. (18)) which yields to

$$N_x^0 = -\frac{c_1 a/2 + c_2}{1-\nu}(\Delta T_C G_3 + T_m G_1)$$

$$N_y^0 = -\left[c_1 x + \frac{\nu c_1 a}{2(1-\nu)} + \frac{c_2}{1-\nu}\right](\Delta T_C G_3 + T_m G_1) \tag{56}$$

$$N_{xy}^0 = 0$$

In the next step, we substitute $T(z)$ in Eqs. (16) and calculate Θ as

$$\Theta = T_m \int_{-\xi/2}^{\xi/2} E(z)\alpha(z)\,dz + \frac{\Delta T_C}{\hat{C}_0}\int_{-\xi/2}^{\xi/2} L(z)E(z)\alpha(z)\,dz \tag{57}$$

Substituting Eq. (56) into Eq. (27), the buckling equation for this case of loading is obtained. By performing an analysis similar to that given for the case A, the thermal critical buckling load, ΔT_C^{cr}, for case C is determined to be

$$\Delta T_C^{cr} = \frac{\pi^2[(b/a)^2+1]}{b^2(1+\nu)(c_1 a/2 + c_2)G_3}\left\{(\widetilde{C} - \widetilde{B}^2/\widetilde{A})(c_1^3 a^3/4 + c_1^2 c_2 a^2 + 3c_1 c_2^2 a/2 + c_2^3)\right.$$

$$\left. + 6(\widetilde{C} - \widetilde{B}^2/\widetilde{A})\frac{a^2 b^2(b^2 + \nu a^2)}{\pi^2(b^2+a^2)^2}(c_1^3 a/2 + c_1^2 c_2)\right\} - \frac{T_m G_1}{G_3} \tag{58}$$

in which

$$G_3 = 1/\hat{C}_0 \{E_m\alpha_m[1/2 - K_{cm}/(k+2)(k+1)K_m + K_{cm}^2/(2k+2)(2k+1)K_m^2 -$$
$$K_{cm}^3/(3k+1)(3k+2)K_m^3 + K_{cm}^4/(4k+2)(4k+1)K_m^4 - K_{cm}^5/(5k+2)(5k$$
$$+1)K_m^5] + (E_m\alpha_{cm} + E_{cm}\alpha_m)[1/(k+2) - K_{cm}/(2k+2)(k+1)K_m + K_{cm}^2$$
$$/(3k+2)(2k+1)K_m^2 - K_{cm}^3/(4k+2)(3k+1)K_m^3 + K_{cm}^4/(5k+2)(4k+1)$$
$$K_m^4 - K_{cm}^5/(6k+2)(5k+1)K_m^5] + E_{cm}\alpha_{cm}[1/(2k+2) - K_{cm}/(3k+2)(k+1)$$
$$k_m + K_{cm}^2/(2k+1)(4k+2)K_m^2 - K_{cm}^3/(5k+2)(3k+1)K_m^3 + K_{cm}^4/(6k+$$
$$2)(4k+1)K_m^4 - K_{cm}^5/(7k+2)(5k+1)K_m^5]\} \tag{59}$$

when $c_1 = 0$, Eq. (58) will reduced to the critical buckling load $\Delta T_{C_i}^{cr}$ of a FGM rectangular plate with constant thickness $c_2 = h$, which is

$$\Delta T_{C_i}^{cr} = \frac{\pi^2(A \cdot C - B^2)}{b^2(1+\nu)A \cdot h \cdot G_3}[(b/a)^2 + 1] - \frac{T_m G_1}{G_3} \tag{60}$$

The result given in Eq. (60) is exactly the same as the one obtained by Ref. [9].

6   RESULTS AND DISCUSSIONS

In this paper, the pre-buckling and critical thermal buckling loads of a thin rectangular FGM plate with variable thickness are obtained. Thickness variation follows simultaneously with two different types of linear changes both in x and y directions, respectively. In order to conduct further calculations, a functionally graded material consisting of aluminum and alumina is considered in which the Young's modulus, conductivity, and the coefficient of thermal expansion, are: for the aluminum, $E_m = 70$ GPa, $K_m = 204$ W/mK , $\alpha_m = 23\times10^{-6}$ (1/$^{\circ}$ C) and for the alumina, $E_c = 380$ Gpa, $K_c = 10.4$ W/mK, $\alpha_c = 7.4\times10^{-6}$ (1/$^{\circ}$ C) and $\nu_m = \nu_c = 0.3$ for both. The critical temperature change ΔT^{cr} versus the aspect ratio b/a, c_1, and volume fraction exponent k for two types of linear change of thickness at x, y directions and three types of thermal loadings are shown in Figs. 2-13. To begin with, we start with the variation of the critical temperature difference ΔT_A^{cr} of FGRP under uniform temperature rise vs. different geometric parameter (b/a), for different volume fraction exponent. The variations are plotted in Figs. 2-5.
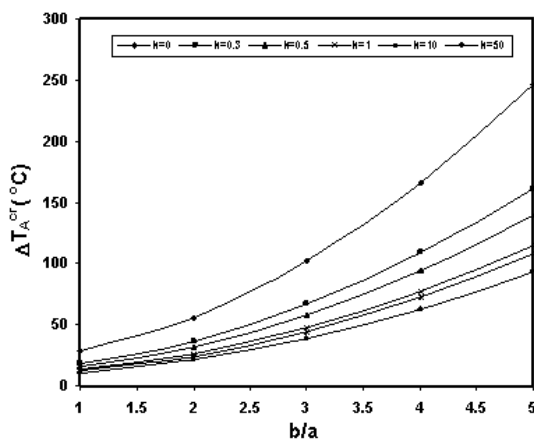

Fig.2
Variation of buckling critical temperature gradient vs. b/a for different FGRP with linear thickness change in x direction under uniform temperature rise (c_1, c_2 =const.).
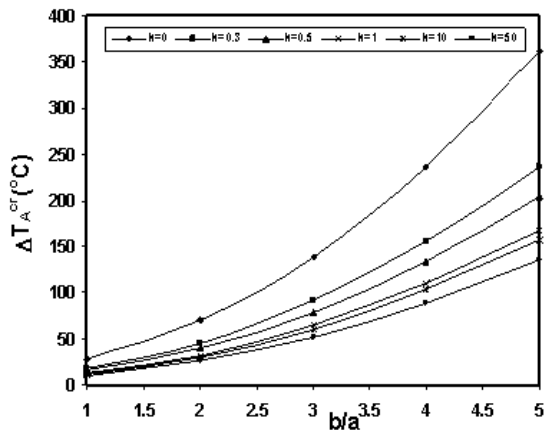
Fig.3
Variation of buckling critical temperature gradient vs. *b/a* for different FGRP with linear thickness change in *y* direction under uniform temperature rise (c_1, c_2 =const.).
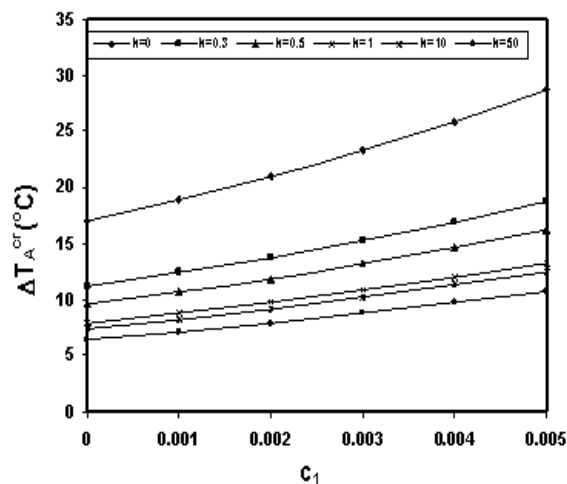

Fig.4
Variation of buckling critical temperature gradient vs. c_1 for different FGRP with linear thickness change in both *x* and *y* directions and under uniform temperature rise (b/a =1, c_2 =const.).

By comparing the values of the critical temperature differences ΔT_A^{cr} calculated with using linear change in the plate thickness at the *x* direction are lower than *y* direction. For the plate of FGM material (*k*>0), the critical temperature difference of the buckling for thickness variation in the *y*-direction is higher than of *x*-direction. Therefore, the plate strength against buckling with respect to all kinds of thermal loads is higher in *y*-direction when the plate has a variable thickness. Fig. 4 illustrates the variation of the buckling critical temperature gradient of different FGRP versus thickness variation parameter c_1 for the linear change in the plate thickness in both *x* and *y* directions subjected to uniform temperature rise when *b/a* =1 and c_2 = constant. Notice that ΔT_A^{cr} has a shallow increase specially for $k \geq 0$. Moreover, *k*=0 represents a fully ceramic plate. Fig. 5 displays the variation of the buckling critical temperature gradient, ΔT_A^{cr} vs. the material index *k* for a FGRP with linear thickness change in both *x* and *y* directions under uniform temperature rise when *b/a* =1, c_2 =const. From Fig. 5 we can see that unlike the former case, the critical temperature difference demonstrates a decreasing trend with increasing gradient index *k*. It is evident that ΔT_A^{cr} changes very slowly when the material gradient index *k* is greater than 1. Moreover, again *k*=0 represents a fully ceramic plate. In Figs. 6-9 the graphs of buckling critical temperature gradient of different FGRP's under linear temperature change across the thickness vs. different types of geometric parameter and volume fraction exponent *k*, are plotted. Fig. 9 demonstrates the variation of buckling critical temperature ΔT_B^{cr} vs. the material graded index *k*. From Fig. 9 we can see that unlike the former cases, the critical temperature difference

demonstrates a decreasing trend with increasing gradient index. It is evident that ΔT_B^{cr} changes very slowly or constant when the material gradient k is greater than 10.
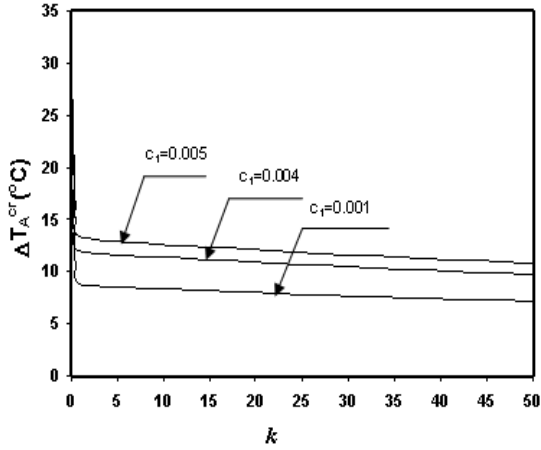

Fig. 5
Variation of the buckling critical temperature gradient *vs.* material index *k* for different FGRP with linear thickness change in *x* and *y* directions under uniform temperature rise (b/a =1, c_2 =const.).
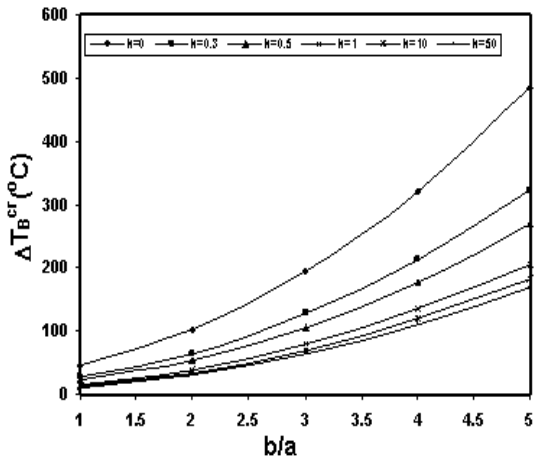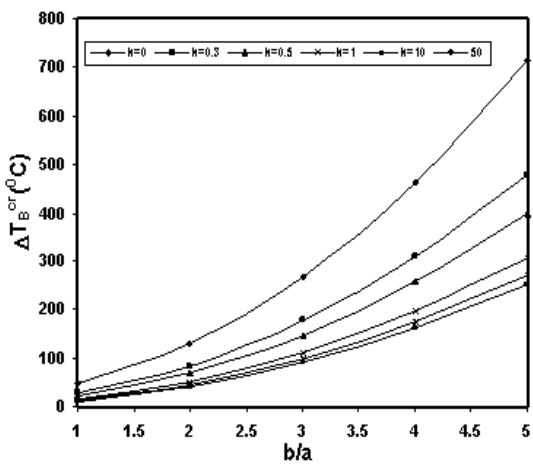

Fig. 6
Variation of the buckling critical temperature gradient vs. *b/a* for different FGRP with linear thickness change in *x* direction under linear temperature change across the thickness (c_1, c_2 =const.).
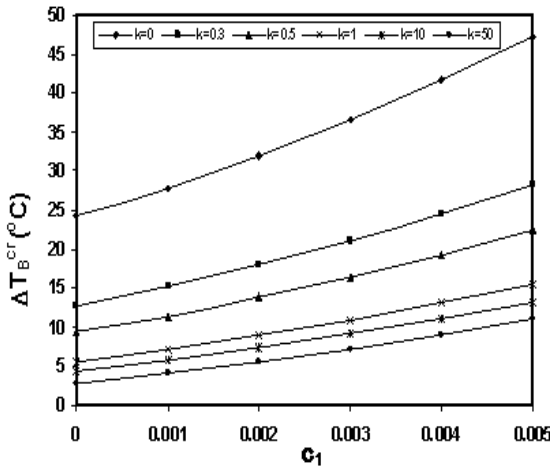

Fig. 7
Variation of the buckling critical temperature gradient vs. *b/a* for different FGRP with linear thickness change in *y* direction under linear temperature change across the thickness (c_1, c_2 =const.).

186   *M. Pouladvand*

Fig. 8
Variation of the buckling critical temperature gradient vs. c_1 for different FGRP with linear thickness change in x and y directions under linear temperature change across the thickness (b/a=1, c_2 =const.).
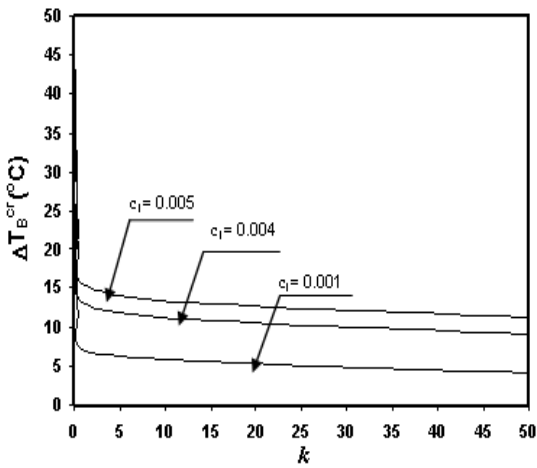

Fig. 9
Variation of the buckling critical temperature gradient vs. material index k for different FGRP with linear thickness change in both x and y directions under linear temperature across thickness (b/a =1).
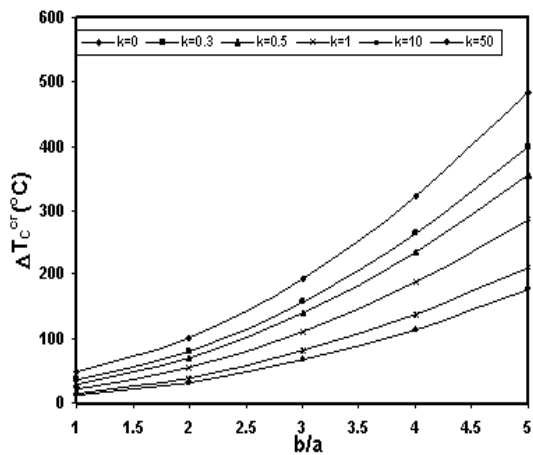

Fig. 10
Variation of the buckling critical temperature gradient vs. b/a for different FGRP with linear thickness change in x direction under non-linear temperature rise across the thickness (c_1, c_2 =const.).

In Figs. 10-13 the graphs of buckling critical temperature gradient of FGRP under non-linear temperature change across the thickness versus two types of different geometric parameter and volume fraction exponent k, are plotted.
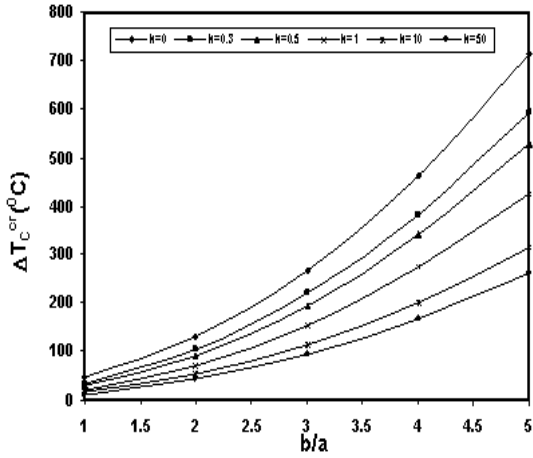
Fig. 11
Variation of the buckling critical temperature gradient vs. b/a for different FGRP with linear thickness change in y direction under non-linear temperature rise across the thickness (c_1, c_2 =const.).
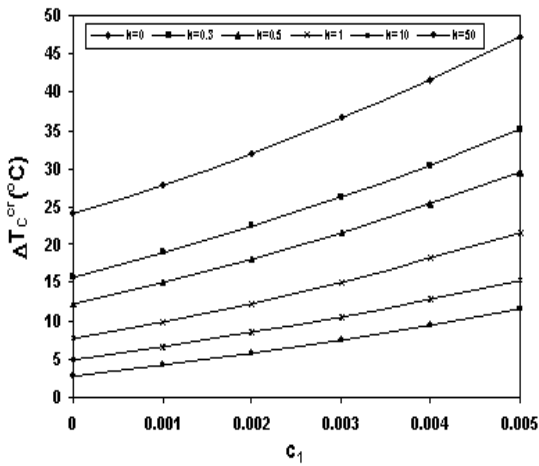

Fig. 12
Variation of the buckling critical temperature gradient vs. c_1 for different FGRP with linear thickness change in x and y directions under non-linear temperature change across the thickness (b/a =1, c_2 =const.).

Fig. 13
Variation of the buckling critical temperature gradient vs. material index k for different FGRP with linear thickness change in both x and y directions under non-linear temperature across thickness (b/a =1).
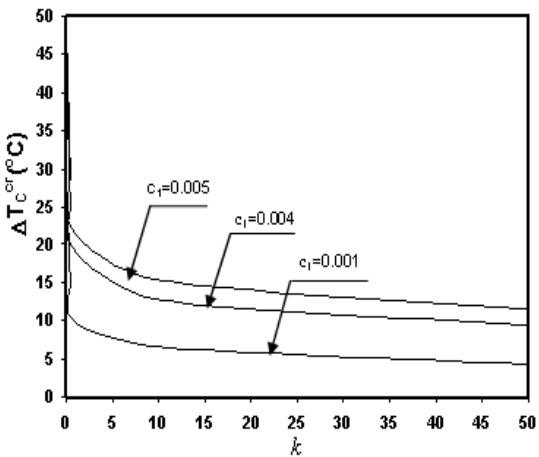
In Fig. 13 variation of the buckling critical temperature gradient vs. material index k for different FGRP with linear thickness change in both x and y directions under non-linear temperature across thickness when b/a =1 is plotted. As it is seen in this figure, the critical temperature gradient has the highest variation for the range of $0<k<10$

and for k values greater than 10 it flattens and reaches to a steady state condition. In an overview of all above cases, one can say that the buckling critical temperature gradient of a homogeneous ceramic plate (k=0), is higher than the FGM plate. This result is justifiable, because the coefficient of the thermal expansion of ceramic plate is lower than the FGM plate. Referred to Figs. 10-11 it can be said that the difference between variation of buckling critical temperature gradient of the homogeneous ceramic plate (k=0) and the FGM plate (k>0) is not significantly high but rather small. Contrary to this, on the other types of loadings the difference is much higher; therefore, this type of loading results in a more acceptable thermal stress distribution in the plate. In Figs. 2-13, it is found that the critical temperature difference of FGRP is higher than that of the fully metal plate but lower than that of the fully ceramics plate. In addition, the critical temperature change decreases as volume fraction exponent k is increased. In all cases, the critical temperature difference increases, when the geometric parameter b/a is increased.

6   CONCLUSIONS

In the present paper, equilibrium and stability equations for a simply supported rectangular functionally graded plate with its thickness varying along both the x and y axes as a linear function, under thermal loading are obtained according to the classical plate theory. The buckling critical temperature gradient for three different types of thermal loadings is derived using Galerkin method. From the obtained results, primarily one can conclude that the thickness change causes the reinforcement or reduction of the load-carrying capacity of plate structure. So, this effect should be taken into account in the engineering design of plate structures. Moreover, based on the analysis of numerical results, the following conclusions are reached:

1. The critical buckling temperature difference ΔT^{cr} for FGRP are generally lower than the corresponding values for homogeneous ceramic plate (k=0).

2. The critical buckling temperature difference ΔT^{cr} for a FGRP will increase as b/a and c_1 increase.

3. The critical buckling temperature difference $\Delta T^{cr}_{A,B,C}$ for a FGRP is decreasing the volume fraction exponent k increases.

4. The critical buckling temperature difference ΔT^{cr} for FGRP with a linear thickness change in x direction is lower than the one for the plate with a linear thickness change in y direction.

5. The critical buckling temperature difference ΔT^{cr} increases steadily as c_1 increases. This indicates that no sudden variation can occur on the critical buckling load under this condition hence, it can be regarded as an advantage.

6. The difference between variation buckling critical temperature gradient of the homogeneous ceramic plate (k=0) and the FGM plate (k>0) is not significantly high but rather small. Contrary to this, on the other types of loadings the difference is much higher; therefore, this type of loading results in a more acceptable thermal stress distribution in the plate.

7. For the nonlinear type of loading in z-direction, the plate experiences a thermal stress distribution which is lower than the one induced by two other linear types.

REFERENCES

[1]   Koizumi M., 1997, FGM activities in Japan, *Composites part B: Engineering* **28**(1-2): 1-4.
[2]   Fuchiyama T., Noda N., 1995, Analysis of thermal stress in a plate of functionally gradient material, *JSME Review* **16**: 263-269.
[3]   Tanigawa Y., Matsumoto M., Akai T., 1997, Optimization of material composition to minimiza thermal stresses in non-homogeneous plate subjected to unsteady heat supply, *JSME International Journal Series A-Solid Mechanics and Material Engineering* **40**(1): 84-93.
[4]   Takezono S., Tao K., Inamura E., 1996, Thermal stress and deformation in functionally graded material shells of revolution under thermal loading due to fluid, *JSME International Journal Series A-Solid Mechanics and Material Engineering* **62**(594): 474-481.
[5]   Aboudi J., Pindera M., Arnold S.M., 1995, Coupled higher-order theory for functionally grade composites with partial homogenization, *Composites part B: Engineering* **5**(7): 771-792.
[6]   Reddy J.N., Chin C.D., 1998, Thermomechanical analysis of functionally graded cylinders and plates, *Journal of Thermal Stresses* 2: 593-626.

[7] Reddy J.N., Cheng Z.Q., 2001, Three-dimensional thermomechanical deformations of functionally graded rectangular plates, *European Journal of Mechanics A/Solids* 20: 841-855.

[8] Cheng Z.Q., Batra R.C., 2000, Three-dimensional thermoelastic deformations of a functionally graded elliptic plate, *Composites part B: Engineering* **31**: 97-106.

[9] Javaheri R., Eslami M.R., 2002, Thermal buckling of functionally graded plates, *AIAA Journal* **40**(1): 162-169.

[10] Javaheri R., Eslami M.R., 2002, Thermal buckling of functionally graded plates based on higher order theory, *Journal of Thermal Stresses* **25**(7): 603-625.

[11] Najafizadeh M.M., Eslami M.R., 2002, First order theory based thermoelastic stability of functionally graded material circular plates, *AIAA Journal* **40**: 1444-1450.

[12] Najafizadeh M.M., Heydari H.R., 2004, Thermal buckling of functionally graded circular plates based on higher order shear deformation plate theory, *European Journal of Mechanics A/Solids* **23**: 1085-1100.

[13] Wetherhold R.C., Seelman S., Wang J., 1996, The use of functionally graded materials to eliminate or control thermal deformation, *Composite Science and Technology* **56**: 1099-1104.

[14] Tanigawa Y., Morishita H., Ogaki S., 1999, Derivation of system of fundamental equations for a three dimensional thermoelastic field with non-homogeneous material properties and its application to a semi-infinite body, *Journal of Thermal Stresses* **22**: 689-711.

[15] Praveen G.N., Reddy J.N., 1998, Nonlinear transient thermoelastic analysis of functionally graded ceramic-metal plates, *International Journal of Solids and Structures* **35**: 33: 4457-4476.

[16] Brush D.O., Almroth B.O., 1975, *Buckling of Bars, Plate and Shell*, McGraw Hill, New York.